analytical chemistry

pubs.acs.org/ac Letter

Development of Dual-Nanopore Biosensors for Detection of Intracellular Dopamine and Dopamine Efflux from Single PC12 Cell

Tao Zhao, Jing-Wen Wang, Hong-Shuai Zhang, Xin Zheng, Yi-Ping Chen, Hao Tang,* and Jian-Hui Jiang

Cite This: https://doi.org/10.1021/acs.analchem.2c04050 Read Online

ACCESS | Metrics & More | Article Recommendations | Supporting Information

ABSTRACT: Detection of neurotransmitters at the single-cell level is essential for understanding the related biological processes and neurodegenerative diseases. We report a dual-nanopore biosensor utilizing a DNA aptamer probe to specifically interact with dopamine, enabling detection of intracellular dopamine and dopamine efflux (extracellular dopamine) in a single pheochromocytoma (PC12) cell. We demonstrate the ability to form an intrapipette electric circuit with the dual-nanopore configuration, which is crucial to achieving both intracellular and extracellular dopamine detection. The sensor allowed rapid detection of dopamine in 10 min with a limit of detection of 0.4 nM. We show the dual-nanopore biosensor was able to monitor single-cell dopamine concentration change under different stimulations. The developed dual-nanopore biosensor represents a novel strategy for time-dependent monitoring of neuron behavior at the single-cell level and potentially can be extended to other platforms for single-cell analysis.

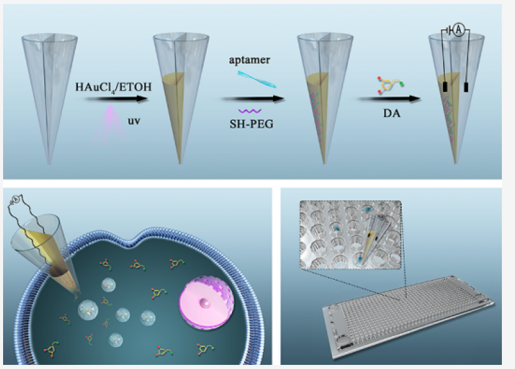

Downloaded via 143.137.155.56 on November 10, 2022 at 08:25:51 (UTC).
See https://pubs.acs.org/sharingguidelines for options on how to legitimately share published articles.

INTRODUCTION

Neurotransmitters such as dopamine, acetylcholine, epinephrine, norepinephrine, etc. play crucial functions in neural communication and are closely related to various neurodegenerative diseases.[1,2] Techniques that enable spatiotemporally resolved monitoring of neurotransmitters in single living cell levels are of crucial importance for investigation of neurotransmitter-related biological processes and diseases.

Nanoelectrodes/nanopipettes are valuable tools for single-cell electrochemical analysis because they can be placed inside or near a single cell with high spatial resolution.[3,4] They have been successfully demonstrated for use in single-cell neurotransmitter detection, including the detection of concentration change inside live cells or secretion of neurotransmitter from a single cell.[5,6] Nevertheless, these methods mainly rely on a redox reaction to generate current signals, while the oxidation potentials of these neurotransmitters may overlap with each other and electroactive molecules inside or outside the cell to cause interference.[7] Utilizing an aptamer as a recognition element for dopamine, a silicon nanowire field-effect transistor device modified with a DNA aptamer demonstrated high-selectivity detection of dopamine secretion from single living PC12 cells over other neurotransmitters such as epinephrine and norepinephrine.[8] However, the field-effect transistor device requires a sophisticated fabrication process and is not suitable for intracellular detection.

Our recent work demonstrated that the novel design of a dual-nanopore biosensor had unique advantages for single intracellular analysis compared to a single nanopipette biosensor because the intrapipette electric circuit eliminates interference from the cell membrane.[9] Herein, we have expanded the application of dual-nanopore biosensors for the detection of targets from single-cell secretion. We have chosen dopamine as a model target and PC12 cells for demonstration because dopamine is a well-known and important neurotransmitter involved in motor and cognitive functions and abnormal levels of dopamine have been correlated with various diseases, including schizophrenia, Huntington's disease, and Parkinson's disease.[1,10,11] The principle of our dual-nanopore biosensor for dopamine detection is demonstrated in Figure 1. We chose a DNA aptamer that specifically binds with dopamine to be modified onto the nanopore surface.[8,12,13] The thiol modified DNA aptamer (the sequence is listed in the Experimental Section in the Supporting Information) was assembled onto one nanopore deposited with a gold film. The interaction between DNA aptamers and positively charged dopamine molecules would induce partial neutralization of the negative surface charge (Figure 1A). The ionic current in the nanopore was closely correlated to its surface charge, and ionic

Received: September 14, 2022
Accepted: November 2, 2022

© XXXX American Chemical Society

https://doi.org/10.1021/acs.analchem.2c04050
Anal. Chem. XXXX, XXX, XXX−XXX

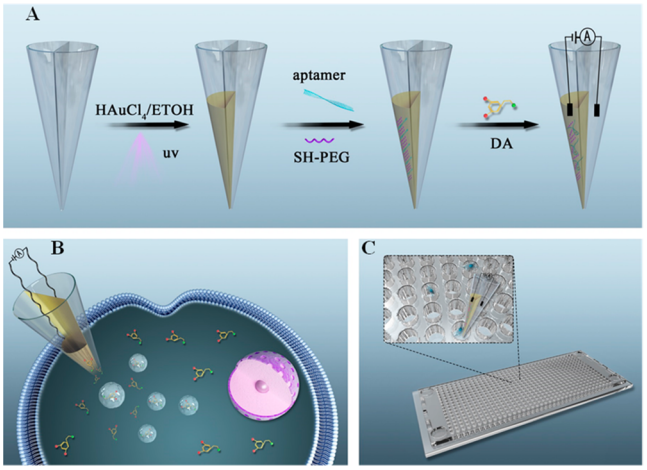

Figure 1. (A) Illustration of the dual-nanopore biosensor for dopamine detection based on DNA aptamer recognition. (B) Dual-nanopore biosensor for single-cell dopamine detection. (C) The detection of single-cell dopamine secretion utilizing dual-nanopore biosensor and a microwell array chip.

current rectification (ICR) occurs in asymmetric nanopore structures to generate potential-dependent ion fluxes.[14] Hence, the concentration of the dopamine target could be correlated with the measured ionic current amplitude decrease. The dual-nanopore biosensor can be positioned in a single cell to monitor intracellular dopamine levels, and this architecture forms an intrapipette electric circuit to exclude the cell membrane (Figure 1B). Moreover, given the advantage of the intrapipette electric circuit of the dual-nanopore biosensor, we can realize the monitoring of dopamine secretion from a single cell with a microwell array chip (Figure 1C). The design of the microwell (~100 μm diameter and ~50 μm depth) can entrap a single PC12 cell and enable a relatively high concentration of secreted dopamine due to the confined small volume (~390 pL).

The dual-nanopore structure was fabricated from a dual barrel of a quartz capillary by a laser pulling process.[15] The diameters of the two pores were ~50 nm, which were characterized by scanning electron microscopy (SEM) (Figure 2A). Then the fabricated dual nanopore was utilized to prepare the dopamine biosensor via deposition of a gold film and self-assembly of DNA aptamers on the inner surface of one nanopore. The deposition of the gold film was validated by SEM elemental mapping and UV−vis absorption spectrum (Figures S1 and S2). After the assembly of DNA aptamers, the inner surface of the nanopore was blocked with mPEG-thiol 2000 to minimize nonspecific adsorption. The other nanopore with a quartz surface was also blocked with silane-PEG. The assembly processes of the pore surface were characterized by ionic current rectification (ICR) responses (Figure 2B). The bare dual nanopore without modification presented a typical ohmic response with no ICR effect because the surfaces of the two nanopores had similar negative surface charges.[16] The gold film deposition in one nanopore surface resulted in a prominent ICR response due to the increased negative surface charge because chloride ions could form a chemisorption bond with the gold surface.[17] The self-assembly of DNA aptamers led to further promotion of the ICR, because the DNA phosphate backbones were deprotonated at neutral conditions and could increase the negative surface charge. The slight decrease of ICR after PEG blocking might be attributed to

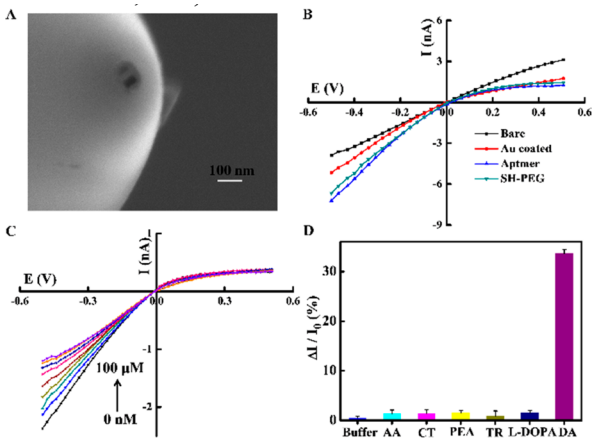

Figure 2. (A) Typical SEM images of dual-nanopore structure. (B) ICR responses in $I-V$ curve of the dual nanopore after different modification processed on the inner surface with two barrels filled with 1× PBS. (C) $I-V$ curves of dual-nanopore biosensor responding to different dopamine concentrations (0, 1 nM, 5 nM, 10 nM, 50 nM, 100 nM, 1 μM, 10 μM, and 100 μM) with two barrels filled with 0.1× PBS. (D) Selectivity investigation of dual-nanopore biosensor with 1 μM dopamine and different interferents at 10 μM.

replacement of DNA aptamers. These results confirmed the successful establishment of our biosensors in each step.

The ability of the developed biosensor to detect dopamine was investigated in 1× PBS (pH 7.4) electrolyte, which is similar to the physiological environment. Utilizing a linear sweep voltammetry setting between −0.4 and 0.4 V, the ionic current recorded at −0.4 V decreased monotonically upon the addition of an increasing concentration of dopamine from 1 to 100 μM (Figure S3). Moreover, the biosensor responded to dopamine rapidly; the ionic current decrease reached ~90% in 5 min and a plateau in 10 min. (Figure S4). This result could be attributed to the chargeability of dopamine, because dopamine had a pK_a of 8.87 and the amine group of dopamine was positively charged at pH 7.4.[18] Hence, the negative charges on the nanopore surface would be subsequently partially neutralized by the amine group of dopamine after binding with the DNA aptamer,[8,13,19] leading to a decrease in the rectified ionic current. We have utilized the nanopore sensor to detect dopamine with different electrolyte concentrations of 0.1× PBS, 1× PBS, and 10× PBS; the ionic current response became smaller with the increase of electrolyte concentration, indicating negative surface charge decrease induced by binding of dopamine with DNA aptamer (Figure S5). To further clarify that the ionic current response was due to the specific binding of aptamer and dopamine, we performed a control experiment to investigate the ionic current responses toward dopamine of nanopores with different surface properties. Only negligible ionic current responses were observed for 10 μM dopamine with bare nanopore, gold film-coated nanopore, or random DNA-modified nanopore, while the nanopore biosensor modified with DNA aptamers showed distinct ionic current response (Figure S6).

Because of the low concentration of intracellular and extracellular dopamine, improvement of the sensitivity of the biosensor could be important. According to a previous study of the ICR phenomenon, a decrease of nanopore size or electrolyte concentration might be able to improve the ionic current response because these methods could reduce the difference between the nanopore diameter and Debye

https://doi.org/10.1021/acs.analchem.2c04050
Anal. Chem. XXXX, XXX, XXX−XXX

screening length.[20] It was reported that electrostatic interactions of the mobile ions with fixed surface charges will result in an increase of the normalized current rectification as the electrolyte concentration decreased.[21,22] Hence, a lower electrolyte concentration (0.1× PBS, pH 7.4) was utilized for dopamine detection because it still could ensure a sufficient ionic strength for dopamine binding to aptamer.[8] The two nanopores were filled with 0.1× PBS buffer and inserted into 1× PBS solution which was similar to the cellular environment. The ionic current was quite stable over time in the absence of dopamine, probably because of the intrapipette electric circuit (Figure S7). The current decreases were dynamically correlated to dopamine concentration ranging from 1 nM to 100 μM utilizing a linear sweep voltammetry method (Figure 2C). A linear relationship between the current amplitude at −0.4 V and the logarithm of dopamine concentrations was obtained from 1 nM to 10 μM with an estimated limit of detection (LOD) of 0.4 nM according to the 3σ rule (Figure S8). The high sensitivity of the biosensor enables single-cell dopamine analysis. We also observed a slight increase of current amplitude decrease with smaller nanopore size (Figure S9), which was consistent with our previous study.[9] Because it becomes increasingly difficulty to pull a controllable pore size and to chemically modify glass nanopipettes when the pore aperture gets too small,[23,24] we chose to construct the dual-nanopore biosensor with a ∼50 nm dual-nanopore structure. The dual-nanopore biosensor showed prominent specific response to 1 μM dopamine (current amplitude $\Delta I/I_0$ of 32.3%), and only negligible current signal changes (<1.6%) were observed in control experiments using other interferents, including ascorbic acid (AA), catechol (CT), phenethylamine (PEA), tyrosine (TR), and 3,4-dihydroxyphenylalanine (L-DOPA) each at concentration of 10 μM (Figure 2D). The regeneration of the nanopore sensor was performed by immersing it in 0.1× PBS (pH 7.4) for 2−4 h to allow the dissociation of dopamine and to restore the nanopore surface with DNA aptamer. The nanopore sensors could be reused 5 times and demonstrated uncompromised sensitivity for dopamine detection for 1 week when stored in refrigerator at 4 °C (Figures S10 and S11)

The dual-nanopore biosensor was controlled using a homemade micromanipulation system for single-cell analysis.[9] We investigated the biocompatibility of the nanopore sensor utilizing propidium iodide (PI), a fluorescence dye that can permeate only those cells with a damaged membrane. Only negligible intracellular fluorescence was observed after insertion of the nanopore sensor for HeLa or PC12 cells for 3 h (Figure S12). The results demonstrated excellent biocompatible of the nanopore sensor, which was consistent with previous reports that insertion of nanoelectrode/nanopore into a single cell resulted in very little damage to different types of cells.[9,23,25−27] Because of the complexity of the cellular environment, we performed control experiments to evaluate the ability of the nanopore biosensor for live cell analysis. When utilizing the nanopore biosensor modified with random DNA but without PEG blocking, distinct ionic current decreases were observed for a single live cell and cell lysate of the PC12 cell line, which was probably due to the decease of effective pore size from nonspecific adsorption of protein molecules. On the other hand, only negligible ionic current changes were observed for nanopores further blocked with PEG, indicating this process could effectively eliminate nonspecific adsorption and result in sensors with desirable antifouling performance for dopamine detection in complicated biological samples including single cells and cell lysates (Figure S13). Then we utilized a nanopore biosensor modified with dopamine aptamer and PEG blocking for single-cell analysis of dopamine. Upon penetration in a PC12 cell utilizing a nanopore sensor, a gradual current decrease appeared and became saturated with a 28% current decrease under −0.4 V after ∼10 min (Figure 3A). The response time of a few

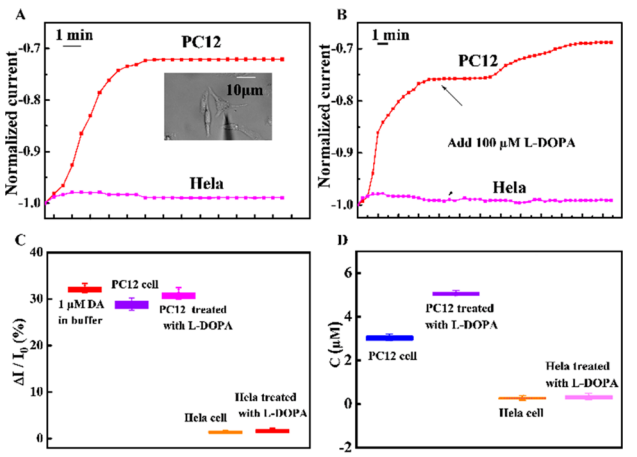

Figure 3. Time-dependent current response to singe-cell dopamine of the nanopore biosensor in cell lines of PC12 and HeLa without (A) or with L-DOPA stimulation (B). (C) Relative single-cell dopamine levels determined by nanopore biosensor in cell lines of PC12 and HeLa without or with L-DOPA stimulation. (D) Relative dopamine levels estimated by a commercial ELISA kit in cell lines of PC12 and HeLa without or with L-DOPA stimulation utilizing cell lysate samples. The time-dependent ionic current responses are normalized to a baseline value of 1.0 by dividing by a constant (initial current value).

minutes can have difficulty in reflecting the real-time change of dopamine level occurring in a few seconds. Nevertheless, for investigation of neurotransmitter-related biology processes and diseases, monitoring of dopamine for a long time scale from minutes to hours under stimulation is as crucial as detecting second/millisecond changes in dopamine concentrations.[5,6,28−30] We expect that the nanopore sensor could have potential for application for long time scale monitoring of dopamine. Only negligible ionic current responses were obtained when utilizing nanopore biosensor inserted into a single HeLa cell (Figure 3A). The results were consistent with previous reports of high dopamine expression in PC12 cell line and nondopamine expression in HeLa cell line.[31,32] Then the nanopore biosensor was utilized to monitor intracellular dopamine level change stimulated with L-DOPA, a direct precursor of dopamine that could pass the cell membrane to increase intracellular dopamine concentration.[5,33] After a stable current response was obtained for the nanopore biosensor in a PC12 cell, a further current decrease was induced by the addition of 100 μM L-DOPA, indicating increased intracellular dopamine level. In contrast, no significant current decrease has been observed with a HeLa cell after adding L-DOPA (Figure 3B). The results were consistent with a report that L-DOPA could induce dopamine biosynthesis in PC12 within 30 min.[33] It is worth mentioning that monitoring of real-time dopamine decrease with the nanopore sensor is not applicable because a high-affinity dopamine aptamer was utilized to achieve high sensitivity for dopamine detection. Nevertheless, by tuning the

https://doi.org/10.1021/acs.analchem.2c04050
Anal. Chem. XXXX, XXX, XXX−XXX

sequence to lower binding affinity, the ability of the sensor to reflect dopamine decrease may be improved, but with a compromised sensitivity.[9] We measured several different single cells (cell number 8) with the nanopore biosensor and found heterogeneous dopamine level in the same PC12 cell line, which was consistent with previous reports of single-cell heterogeneity.[9] The average current responses showed distinct differences in dopamine levels among PC12 cell, HeLa cell, and PC12 cell treated with L-DOPA (Figure 3C). The dopamine concentration in a single PC12 cell was estimated to be ~0.4 μM according to the average current decrease amplitude of 28.9%. The dopamine concentration in a single PC12 cell after L-DOPA stimulation was estimated to be ~0.8 μM according to the average current decrease amplitude of ~31.3%. We also utilized a commercial ELISA kit to measure dopamine concentration in cell lysate with or without L-DOPA treatment. The results revealed no dopamine was detected in HeLa cell lysate. The intracellular dopamine in the single PC12 cell was determined to be ~3.0 μM, and the dopamine concentrate of the single PC12 cell treated with 100 μM L-DOPA for 30 min was ~5.2 μM (Figure 3D), utilizing an average volume of 2 pL (15 μm diameter) for a single PC12 cell for estimation.[9,34] These values were close to the reported values of dopamine concentrations in PC12 cells with or without L-DOPA stimulation determined by HPLC and intracellular patch electrochemistry methods.[32,33]

It is worth noting that the determined intracellular dopamine concentration by the ELISA method via cell lysate was higher than that measured with the nanopore sensor via a single cell. This could be due to a higher concentration of dopamine in the vesicles than in free cytoplasm and because the nanopore biosensor detects only the free cytoplasm dopamine.

In PC12 cells, dopamine is synthesized in the cell and then packaged into vesicles, and exocytosis is an essential cell function in which chemical messengers are released into the extracellular space from intracellular vesicles.[6,35] Therefore, monitoring of the exocytotic dopamine is also highly desired. We utilized a microwell chip to isolate single PC12 cells. The diluted cell suspension solution was added to the chip, and some microwells would entrap a single PC12 cell due to the small cell numbers. Then water immiscible oil could be added to further isolate individual microwells with air. We also investigated the biocompatibility of the microwell entrapment utilizing the fluorescence dye PI. Only negligible intracellular fluorescence was observed after incubating the HeLa or PC12 cell with the microwell chip for 3 h (Figure S14), indicating the negligible damage to the cell with the microwell entrapment.

The dual-nanopore biosensor was placed inside the microwell where a single PC12 cell was entrapped to form an intrapipette electric circuit for detecting dopamine efflux. Under normoxia buffer, the PC12 and HeLa cells all show negligible ionic current responses. In contrast, a distinct ionic current response was observed for a single PC12 cell under hypoxia buffer but still negligible ionic current response for a single HeLa cell (Figure 4). The dopamine efflux from a single PC12 cell under hypoxia buffer was much higher than PC12 and HeLa cells under normoxia buffer. The results were consistent with previous reports that a hypoxia environment could stimulate PC12 cells to release dopamine.[8,29] These results demonstrated that our nanopore biosensor could monitor the dopamine efflux at the single-cell level.

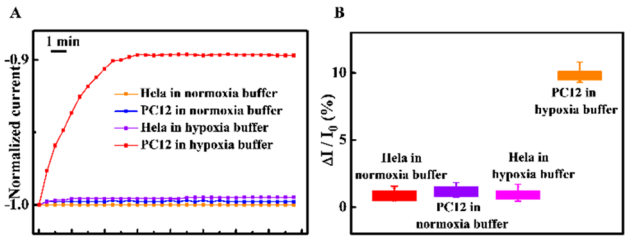

Figure 4. (A) Continuous monitoring of dopamine efflux from single PC12 and HeLa cell under normoxia or hypoxic conditions. (B) Relative dopamine effluxes in PC12 and HeLa cell under normoxia or hypoxic conditions. The time-dependent ionic current responses are normalized to a baseline value of 1.0 by dividing by a constant (initial current value).

CONCLUSION

In conclusion, we have demonstrated dopamine detection at the single-cell level utilizing a dual-nanopore biosensor. Time-dependent monitoring of intracellular dopamine and dopamine efflux (extracellular dopamine) in a PC12 cell has been achieved. This proposed strategy relies on the electrostatic interaction with induced changes of surface charge of the nanopore for rapid detection of small molecules with high sensitivity and selectivity. The developed nanopore sensor has the advantages of low cost and ease of fabrication. The dual-nanopore structure could form an intrapipette electric circuit for ionic current measurement to eliminate possible interference from the cell membrane or in vivo system. It is envisioned that with the progress of advanced micromanipulation instruments, the developed nanopore sensor for high-throughput single-cell analysis may provide a valuable platform for investigation of neurotransmitter-related diseases.

ASSOCIATED CONTENT

Supporting Information

The Supporting Information is available free of charge at https://pubs.acs.org/doi/10.1021/acs.analchem.2c04050.

Experimental details including materials, preparation of nanopore sensors, and assay procedure; Figures S1−S14 (PDF)

AUTHOR INFORMATION

Corresponding Author

Hao Tang − *State Key Laboratory of Chemo/Bio-Sensing and Chemometrics, College of Chemistry and Chemical Engineering, Hunan University, Changsha 410082, P.R. China*; orcid.org/0000-0001-6392-5164; Email: haotang@hnu.edu.cn

Authors

Tao Zhao − *State Key Laboratory of Chemo/Bio-Sensing and Chemometrics, College of Chemistry and Chemical Engineering, Hunan University, Changsha 410082, P.R. China*

Jing-Wen Wang − *State Key Laboratory of Chemo/Bio-Sensing and Chemometrics, College of Chemistry and Chemical Engineering, Hunan University, Changsha 410082, P.R. China*

Hong-Shuai Zhang − *State Key Laboratory of Chemo/Bio-Sensing and Chemometrics, College of Chemistry and Chemical Engineering, Hunan University, Changsha 410082, P.R. China*

https://doi.org/10.1021/acs.analchem.2c04050
Anal. Chem. XXXX, XXX, XXX−XXX

Xin Zheng − *State Key Laboratory of Chemo/Bio-Sensing and Chemometrics, College of Chemistry and Chemical Engineering, Hunan University, Changsha 410082, P.R. China*

Yi-Ping Chen − *State Key Laboratory of Chemo/Bio-Sensing and Chemometrics, College of Chemistry and Chemical Engineering, Hunan University, Changsha 410082, P.R. China*

Jian-Hui Jiang − *State Key Laboratory of Chemo/Bio-Sensing and Chemometrics, College of Chemistry and Chemical Engineering, Hunan University, Changsha 410082, P.R. China;* orcid.org/0000-0003-1594-4023

Complete contact information is available at: https://pubs.acs.org/10.1021/acs.analchem.2c04050

Notes

The authors declare no competing financial interest.

■ ACKNOWLEDGMENTS

This work was supported by NSFC (22090053, 2199108, and 22074037) and CPSF (2021M701146).

■ REFERENCES

(1) Bello, E. P.; Mateo, Y.; Gelman, D. M.; Noaín, D.; Shin, J. H.; Low, M. J.; Alvarez, V. A.; Lovinger, D. M.; Rubinstein, M. *Nat. Neurosci.* **2011**, *14*, 1033.
(2) Chen, W. W.; Zhang, X.; Huang, W. J. *Mol. Med. Rep.* **2016**, *13*, 3391−3396.
(3) Yu, R.-J.; Ying, Y.-L.; Gao, R.; Long, Y.-T *Angew. Chem., Int. Ed.* **2019**, *58*, 3706−3714.
(4) Nascimento, R. A. S.; Özel, R. E.; Mak, W. H.; Mulato, M.; Singaram, B.; Pourmand, N. *Nano Lett.* **2016**, *16*, 1194−1200.
(5) Li, X.; Majdi, S.; Dunevall, J.; Fathali, H.; Ewing, A. G. *Angew. Chem.* **2015**, *127*, 12146−12150.
(6) Liu, Y.; Li, M.; Zhang, F.; Zhu, A.; Shi, G. *Anal. Chem.* **2015**, *87*, 5531−5538.
(7) Li, J.; Li, Y.; Zhang, Y.; Wei, G. *Anal. Chem.* **2012**, *84*, 1888−1893.
(8) Li, B.-R.; Hsieh, Y.-J.; Chen, Y.-X.; Chung, Y.-T.; Pan, C.-Y.; Chen, Y.-T *J. Am. Chem. Soc.* **2013**, *135*, 16034−16037.
(9) Zhang, H.; Zhao, T.; Huang, P.; Wang, Q.; Tang, H.; Chu, X.; Jiang, J. *ACS Nano* **2022**, *16*, 5752−5763.
(10) Wightman, R. M.; May, L. J.; Michael, A. C. *Anal. Chem.* **1988**, *60*, 769A−779A.
(11) Shafer, T. J.; Atchison, W. D. *Neurotoxicology* **1991**, *12*, 473−492.
(12) Walsh, R.; DeRosa, M. C. *Biochem. Biophys. Res. Commun.* **2009**, *388*, 732−735.
(13) Kim, J.; Rim, Y. S.; Chen, H.; Cao, H. H.; Nakatsuka, N.; Hinton, H. L.; Zhao, C.; Andrews, A. M.; Yang, Y.; Weiss, P. S. *ACS Nano* **2015**, *9*, 4572−4582.
(14) Lan, W.-J.; Edwards, M. A.; Luo, L.; Perera, R. T.; Wu, X.; Martin, C. R.; White, H. S. *Acc. Chem. Res.* **2016**, *49*, 2605−2613.
(15) Cadinu, P.; Campolo, G.; Pud, S.; Yang, W.; Edel, J. B.; Dekker, C.; Ivanov, A. P. *Nano Lett.* **2018**, *18*, 2738−2745.
(16) Zhang, S.; Yin, X.; Li, M.; Zhang, X.; Zhang, X.; Qin, X.; Zhu, Z.; Yang, S.; Shao, Y. *Anal. Chem.* **2018**, *90*, 8592−8599.
(17) Xu, X.; He, H.; Jin, Y. *Anal. Chem.* **2015**, *87*, 3216−3221.
(18) Malem, F.; Mandler, D. *Anal. Chem.* **1993**, *65*, 37−41.
(19) Nakatsuka, N.; Yang, K.-A.; Abendroth, J. M.; Cheung, K. M.; Xu, X.; Yang, H.; Zhao, C.; Zhu, B.; Rim, Y. S.; Yang, Y.; Weiss, P. S.; Stojanović, M. N.; Andrews, A. M. *Science* **2018**, *362*, 319−324.
(20) Huang, J.; Sumpter, B. G.; Meunier, V. *Angew. Chem.* **2008**, *120*, 530−534.
(21) Liu, J.; Kvetny, M.; Feng, J.; Wang, D.; Wu, B.; Brown, W.; Wang, G. *Langmuir* **2012**, *28*, 1588−1595.
(22) Liu, J.; Wang, D.; Kvetny, M.; Brown, W.; Li, Y.; Wang, G. *Langmuir* **2013**, *29*, 8743−8752.
(23) Li, Y.; Hu, K.; Yu, Y.; Rotenberg, S. A.; Amatore, C.; Mirkin, M. V. *J. Am. Chem. Soc.* **2017**, *139*, 13055−13062.
(24) Liu, J.; Wang, D.; Kvetny, M.; Brown, W.; Li, Y.; Wang, G. *Anal. Chem.* **2012**, *84*, 6926−6929.
(25) Ying, Y.-L.; Hu, Y.-X.; Gao, R.; Yu, R.-J.; Gu, Z.; Lee, L. P.; Long, Y.-T *J. Am. Chem. Soc.* **2018**, *140*, 5385−5392.
(26) Zhang, X.-W.; Qiu, Q.-F.; Jiang, H.; Zhang, F.-L.; Liu, Y.-L.; Amatore, C.; Huang, W.-H *Angew. Chem.* **2017**, *129*, 13177−13180.
(27) Hu, K.; Le Vo, K. L.; Hatamie, A.; Ewing, A. G. *Angew. Chem.* **2022**, *134*, No. e202113406.
(28) Mohebi, A.; Pettibone, J. R.; Hamid, A. A.; Wong, J. T.; Vinson, L. T.; Patriarchi, T.; Tian, L.; Kennedy, R. T.; Berke, J. D. *Nature* **2019**, *570*, 65−70.
(29) Schwerdt, H. N.; Shimazu, H.; Amemori, K.-i.; Amemori, S.; Tierney, P. L.; Gibson, D. J.; Hong, S.; Yoshida, T.; Langer, R.; Cima, M. J.; Graybiel, A. M. *Proc. Natl. Acad. Sci. U. S. A.* **2017**, *114*, 13260−13265.
(30) Kalmbach, A.; Winiger, V.; Jeong, N.; Asok, A.; Gallistel, C. R.; Balsam, P. D.; Simpson, E. H. *Nat. Commun.* **2022**, *13*, 3805.
(31) Sun, Y.; Pham, A. N.; Waite, T. D. *J. Neurochem.* **2016**, *137*, 955−968.
(32) Mosharov, E. V.; Gong, L.-W.; Khanna, B.; Sulzer, D.; Lindau, M. *J. Neurosci.* **2003**, *23*, 5835.
(33) Jin, C. M.; Yang, Y. J.; Huang, H. S.; Lim, S. C.; Kai, M.; Lee, M. K. *Eur. J. Pharmacol.* **2008**, *591*, 88−95.
(34) Woods, L. A.; Powell, P. R.; Paxon, T. L.; Ewing, A. G. *Electroanalysis* **2005**, *17*, 1192−1197.
(35) Venton, B. J.; Wightman, R. M. *Anal. Chem.* **2003**, *75*, 414A−421A.

https://doi.org/10.1021/acs.analchem.2c04050
Anal. Chem. XXXX, XXX, XXX−XXX